Dual-lobe reconnection and horse-collar auroras

Stephen E. Milan[1], Jennifer Alyson Carter[1], Gemma E. Bower[1], Suzanne Mary Imber[1], Larry J. Paxton[2], Brian J. Anderson[3], Marc R. Hairston[4], and Benoit Hubert[5]

[1]University of Leicester
[2]Johns Hopkins University
[3]John Hopkins Univ.
[4]University of Texas at Dallas
[5]University of Liege

November 21, 2022

Abstract

We propose a mechanism for the formation of the horse-collar auroral configuration during periods of strongly northwards interplanetary magnetic field, invoking the action of dual-lobe reconnection (DLR). Auroral observations are provided by the Imager for Magnetopause-to-Auroras Global Exploration (IMAGE) satellite and spacecraft of the Defense Meteorological Satellite Program (DMSP). We also use ionospheric flow measurements from DMSP and polar maps of field-aligned currents (FACs) derived from the Active Magnetosphere and Planetary Electrodynamics Response Experiment (AMPERE). Sunward convection is observed within the dark polar cap, with antisunwards flows within the horse-collar auroral region, together with the NBZ FAC distribution expected to be associated with DLR. We suggest that newly-closed flux is transported antisunwards and to dawn and dusk within the reverse lobe cell convection pattern associated with DLR, causing the polar cap to acquire a teardrop shape and weak auroras to form at high latitudes. Horse-collar auroras are a common feature of the quiet magnetosphere, and this model provides a first understanding of their formation, resolving several outstanding questions regarding the nature of DLR and the magnetospheric structure and dynamics during northwards IMF. The model can also provide insights into the trapping of solar wind plasma by the magnetosphere and the formation of a low-latitude boundary layer and cold, dense plasma sheet.

Dual-lobe reconnection and horse-collar auroras

S. E. Milan[1,2*], J. A. Carter[1], G. E. Bower[1], S. M. Imber[1], L. J. Paxton[3], B. J. Anderson[3], M. R. Hairston[4], and B. Hubert[5]

[1]School of Physics and Astronomy, University of Leicester, Leicester, UK.
[2]Birkeland Centre for Space Sciences, University of Bergen, Norway.
[3]Johns Hopkins University Applied Physics Laboratory, USA.
[4]William B. Hanson Center for Space Sciences, University of Texas at Dallas, USA.
[5]Laboratory of Planetary and Atmospheric Physics, University of Liège, Liege, Belgium.

Key Points:

- We propose that horse-collar auroras, which occur during prolonged periods of northward IMF, are a signature of dual-lobe reconnection
- The dayside polar cap is eroded and replaced by magnetic flux newly-closed by dual-lobe reconnection, filled with sun-aligned arcs
- Implications for many NBZ phenomena, including solar wind capture, the low-latitude boundary layer, and the cold, dense plasma sheet

*Department of Physics and Astronomy, University of Leicester, Leicester LE1 7RH, UK

Corresponding author: Steve Milan, `steve.milan@le.ac.uk`

Abstract

We propose a mechanism for the formation of the horse-collar auroral configuration during periods of strongly northwards interplanetary magnetic field, invoking the action of dual-lobe reconnection (DLR). Auroral observations are provided by the Imager for Magnetopause-to-Auroras Global Exploration (IMAGE) satellite and spacecraft of the Defense Meteorological Satellite Program (DMSP). We also use ionospheric flow measurements from DMSP and polar maps of field-aligned currents (FACs) derived from the Active Magnetosphere and Planetary Electrodynamics Response Experiment (AMPERE). Sunward convection is observed within the dark polar cap, with antisunwards flows within the horse-collar auroral region, together with the NBZ FAC distribution expected to be associated with DLR. We suggest that newly-closed flux is transported antisunwards and to dawn and dusk within the reverse lobe cell convection pattern associated with DLR, causing the polar cap to acquire a teardrop shape and weak auroras to form at high latitudes. Horse-collar auroras are a common feature of the quiet magnetosphere, and this model provides a first understanding of their formation, resolving several outstanding questions regarding the nature of DLR and the magnetospheric structure and dynamics during northwards IMF. The model can also provide insights into the trapping of solar wind plasma by the magnetosphere and the formation of a low-latitude boundary layer and cold, dense plasma sheet.

Plain Language Summary

During quiet geomagnetic conditions, the global distribution of auroras can acquire a "horse-collar" configuration, in which regions of weak auroral emission appear at dawn and dusk polewards of the main auroral oval. We propose a new model to explain the formation of this configuration, which provides new insights into magnetospheric dynamics during periods of northwards-directed interplanetary magnetic field. To support our proposal, we use observations of the auroras, ionospheric convection, and estimations of the pattern of electrical currents flowing between the ionosphere and magnetosphere from a suite of spacecraft. Our proposed model resolves a 40 year-old question regarding the nature of the horse-collar auroras and many other aspects of magnetospheric dynamics.

1 Introduction

It has been known since space-based auroral imagery was first available that during prolonged periods of northwards-directed interplanetary magnetic field (IMF) the auroral oval can resemble a "horse-collar" and the usually round polar cap becomes teardrop-shaped (e.g. Hones Jr et al., 1989). Figure 1 compares the location of the main auroral oval for active geomagnetic conditions with that which can arise during persistent quiet times. During quiet times the oval contracts to higher latitudes and the dawn and dusk sectors contain weak (even sub-visual) auroras poleward of the main oval. The location of the polar cap boundary, which delineates regions of open field lines at high latitudes and closed field lines, is shown in red. Although this is a common occurrence, to date the cause has not been satisfactorily elucidated: it is the aim of this paper to explain the formation of the horse-collar auroras (HCAs), and by doing so provide a unifying picture of many northward IMF (NBZ) phenomena, including polar cap arcs, cusp auroras, and lobe reconnection.

Auroral features that appear when the north-south component of the IMF is positive ($B_Z > 0$) include polar cap arcs, transpolar arcs, sun-aligned arcs, or bending arcs (see reviews by Zhu et al. (1997), Hosokawa et al. (2020), and Fear (2019)), cusp spots (Milan et al., 2000; Frey et al., 2002; Carter et al., 2020) and high-latitude detached arcs or HiLDAs (Frey, 2007; Carter et al., 2018). Many of these phenomena are understood to be a consequence of magnetic reconnection (Dungey, 1961) occurring in the magnetotail or between the IMF and the high- or low-latitude dayside magnetopause. High-

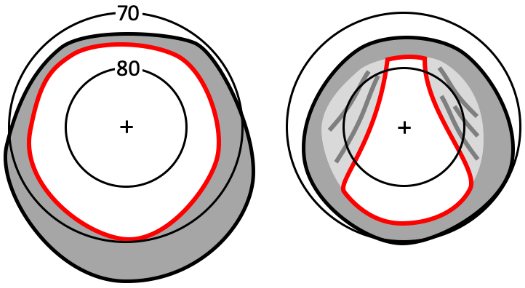

Figure 1. A schematic of the location of the main auroral oval during active conditions (left) and during quiet times (right) when a "horse-collar" auroral morphology can develop, with weak auroras seen at high latitudes in the dawn and dusk sectors and the polar cap (boundary shown in red) becomes teardrop-shaped. The regions of horse-collar auroras can exhibit multiple sun-aligned arcs. Noon is to the top, and circles represent lines of geomagnetic latitude.

latitude reconnection typically occurs between the IMF and the magnetotail lobes, tailwards of the cusps. This is referred to as dual-lobe reconnection (DLR) if the same IMF field line is reconnected with both northern and southern lobes, or single-lobe reconnection (SLR) if the process occurs independently in the two hemispheres (Dungey, 1963; Cowley, 1981). In this paper we argue that horse-collar auroras are a manifestation of dual-lobe reconnection, with significant consequences for our understanding of the large-scale structure and dynamics of the magnetosphere during northwards IMF. We also place the HCAs in the context of the expanding/contracting polar cap model of magnetospheric convection (Cowley & Lockwood, 1992; Milan, 2015) and the other NBZ phenomena mentioned above.

Auroral features contained within the otherwise dark polar cap and approximately aligned parallel to the noon-midnight meridian are a common feature during NBZ conditions. Under the umbrella term "polar cap arcs" (PCAs) these have acquired various names with sometimes only a loose phenomenological (and, until recently, causal) distinction between them. The following taxonomy has slowly developed. "Sun-aligned arcs" (perhaps more accurately called "cusp-aligned arcs" (Y. Zhang et al., 2016)) are relatively dim auroral features which are thought to be produced by field-aligned currents associated with shear flows in the polar cap convection pattern (Hardy et al., 1982; Burke et al., 1982; Carlson & Cowley, 2005; Q.-H. Zhang et al., 2020). Relatively bright "transpolar arcs" (TPAs) or "theta auroras" appear to grow from the nightside auroral oval to almost bisect the polar cap (Frank et al., 1982); after formation these arcs can progress dawnwards and duskwards across the polar cap in response to changes in the east-west (B_Y) component of the IMF. Such arcs have also been argued to be associated with ionospheric convection shears (see discussion in Cumnock and Blomberg (2004)). However, so far the most successful model explaining the formation of TPAs invokes reconnection in a twisted magnetotail producing a tongue of closed magnetic flux that protrudes into the polar cap, and dayside reconnection for the subsequent motion of this flux (Milan et al., 2005; Goudarzi et al., 2008; Fear & Milan, 2012a, 2012b; Fear et al., 2014). The auroral emission of the TPA is produced by precipitation of plasma sheet-like particles trapped in this magnetic field configuration (Fear et al., 2016) which potentially reaches many 10s of Earth radii (R_E) down-tail (Milan et al., 2020). A consequence of their closed nature is that TPAs are expected to occur simultaneously in both northern and southern hemispheres, though there is debate over whether this occurs (Craven et al., 1991; Østgaard et al., 2003; Carter et al., 2017). "Bending arcs" are auroral features that protrude into the polar cap from the dawn- or dusk-side auroral oval and progress over time towards the nightside, which are now thought to be created by low-latitude magnetopause

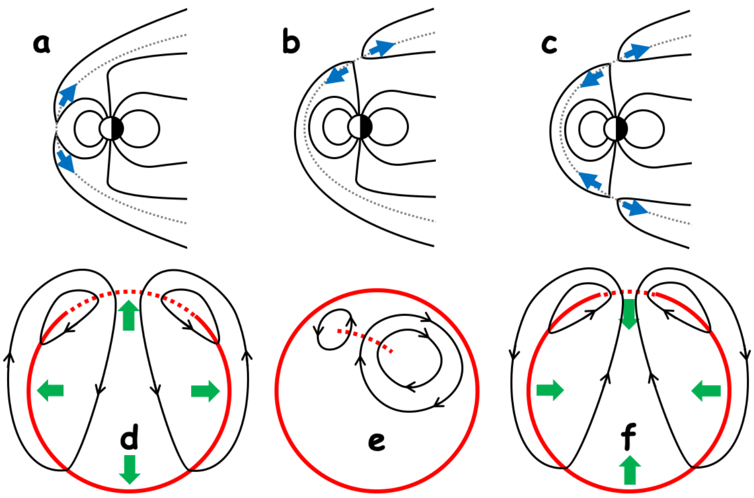

Figure 2. Schematic representations of the cross-section of the magnetosphere when (a) magnetic reconnection is active at the low latitude magnetopause, (b) single-lobe reconnection (SLR) is on-going in the northern hemisphere, and (c) dual-lobe reconnection (DLR) is occurring. Magnetic field lines are shown in black, the location of the magnetopause is the grey dotted line, and blue arrows indicate plasma flows away from the reconnection x-lines. (d) The expected ionospheric flow pattern for low latitude reconnection, IMF $B_Z < 0$, $B_Y \approx 0$. Noon is to the top, and dawn to the right. The red circle indicates the open/closed field line boundary (OCB), with the ionospheric projection of the reconnection x-line shown dotted. Convection streamlines are presented in black. Green arrows indicate the motion of the OCB. (e) Expected flow pattern in the northern hemisphere for SLR, IMF $B_Z > 0$, $B_Y > 0$. (f) The ionospheric flow pattern proposed by Chisham et al. (2004) and Imber et al. (2006) for DLR, IMF $B_Z > 0$, $B_Y \approx 0$. It was assumed that the main auroral oval, at the equatorward edge of the OCB, would also progress polewards with time.

reconnection, in a manner similar to poleward-moving auroral forms associated with flux transfer events, during B_Y-dominated IMF (Carter et al., 2015; Kullen et al., 2002, 2015). Finally, polar cap arcs have been identified as the poleward edge of a thickened plasma sheet in the dawn- and/or dusk-sectors (Meng, 1981; Newell et al., 2009), that is, at the polar cap boundary of the horse-collar auroras, the subject of this paper. At times, polar cap arcs of different origins have been shown to coexist (Reidy et al., 2018, 2020).

When the IMF is directed southwards, low latitude magnetopause reconnection (Figure 2a) causes an increase in the open magnetic flux content of the magnetosphere, an enlargement of the polar caps, with antisunwards flow within the polar caps and sunwards return flow at lower latitudes, often described as the "twin-convection cells" of the Dungey cycle, as sketched in Fig. 2d (Dungey, 1961; Cowley & Lockwood, 1992). Lobe reconnection is noted for producing sunwards-directed ionospheric convection in the noon-sector polar cap, forming "lobe reverse convection cells" (e.g., Reiff, 1982). The exact form of these reverse cells depends on the B_Y component of the IMF, having a dawn-dusk asymmetry if $B_Y \neq 0$ (Reiff & Burch, 1985), shown in Fig. 2b and e. In these cases, lobe field lines in one hemisphere are reconnected with the IMF to become disconnected from the magnetosphere at one end and draped over the nose of the magnetosphere at the other: single-lobe reconnection. Initially, the magnetic tension force on these draped field lines causes sunward convection. Then, the combined action of the magnetosheath flow and B_Y-associated tension forces cause the field lines to be carried around the dawn and dusk flanks of the magnetosphere; whether more flux is carried dawnwards or duskwards, and hence whether the dawn or dusk lobe convection cell dominates, depends on the polarity of B_Y (e.g., Milan et al., 2005): Fig. 2e shows the asymmetry expected in the northern hemisphere for $B_Y > 0$. Two auroral phenomena are associated with lobe reconnection: direct precipitation of magnetosheath plasma along the newly-opened field lines can produce a "cusp spot" downstream of the ionospheric projection of the reconnection site (Milan et al., 2000; Frey et al., 2002; Carter et al., 2020); upwards field-aligned current associated with the vorticity of the dawn lobe cell can produce "high-latitude detached arcs" or HiLDAs (Frey, 2007; Carter et al., 2018). Fig. 2b shows SLR occurring in the northern hemisphere: it can occur simultaneously in the southern hemisphere, though independently and possibly at a different rate.

If $B_Y \approx 0$ it is thought that the same IMF field line can reconnect with both northern and southern lobes (Fig. 2c), eroding open lobe flux and creating newly closed magnetic field lines draped over the nose of the magnetosphere (Dungey, 1963; Cowley, 1981). Chisham et al. (2004) and Imber et al. (2006) argued that this dual-lobe reconnection should produce sunwards ionospheric flow out of the noon-sector polar cap and a contraction of the polar cap as a whole, in both northern and southern hemispheres, as shown in Fig. 2f. Imber et al. (2006, 2007) and Marcucci et al. (2008) did indeed find instances of this occurring, and estimated from observational and theoretical considerations that DLR should occur for IMF clock angles $|\theta| < 10°$, where $\theta = \text{atan2}(B_Y, B_Z)$. The accumulation of closed field lines at the nose of the magnetosphere, possibly mass-loaded with captured solar wind plasma (Sandholt et al., 1999), has then been argued to progress tailwards over time, maybe through a viscous interaction with the magnetosheath flow, and contribute to the formation of the northward IMF "low-latitude boundary layer" or LLBL (e.g., Scholer & Treumann, 1997) and a "cold, dense plasma sheet" or CDPS in the magnetotail (e.g., Terasawa et al., 1997; Øieroset et al., 2005; Imber et al., 2006; Wing et al., 2006; Taylor et al., 2008). Although this aspect of the interaction has received significant attention, there are observational difficulties in its study (a notable exception being Fuselier et al. (2015)). The problem has been further obfuscated by a poor understanding of the range of clock angles over which DLR occurs (Fuselier et al., 2014), the role of viscous processes in mass transport within the magnetosphere (Axford & Hines, 1961), and the possibility that the Kelvin-Helmholtz instability is responsible for the formation of the CDPS by allowing direct entry of solar wind plasma into the flanks of the magnetosphere (Taylor et al., 2008).

We hope to resolve many of these controversies by arguing that the occurrence of dual-lobe reconnection manifests itself in the ionosphere as the formation of horse-collar auroras, providing for the first time a satisfactory mechanism for their production which fits naturally into the scheme developed to explain other facets of magnetospheric dynamics. Our model helps clarify the structural changes that take place in the magnetosphere during periods of NBZ, and facilitates quantification of the rates of dual-lobe reconnection and of solar wind capture by the magnetosphere. The model we propose to replace the picture of Fig. 2f is presented in Figure 3, panels a to c. In this model, the flux newly-closed by DLR is not redistributed equally to all local times, but is added progressively at dawn and dusk, eroding the polar cap to a teardrop shape. The regions of weak auroral emission and sun-aligned arcs forming the horse-collar auroras coincide with the location of newly-closed flux. A key prediction of the model is that sunward ionospheric flows are contained within the remaining polar cap, and antisunwards flows are located in the regions of HCAs. We present observations in support of this model in Section 2. In Section 3 we explain the model in more detail and discuss some of its ramifications. Finally, we conclude in Section 4.

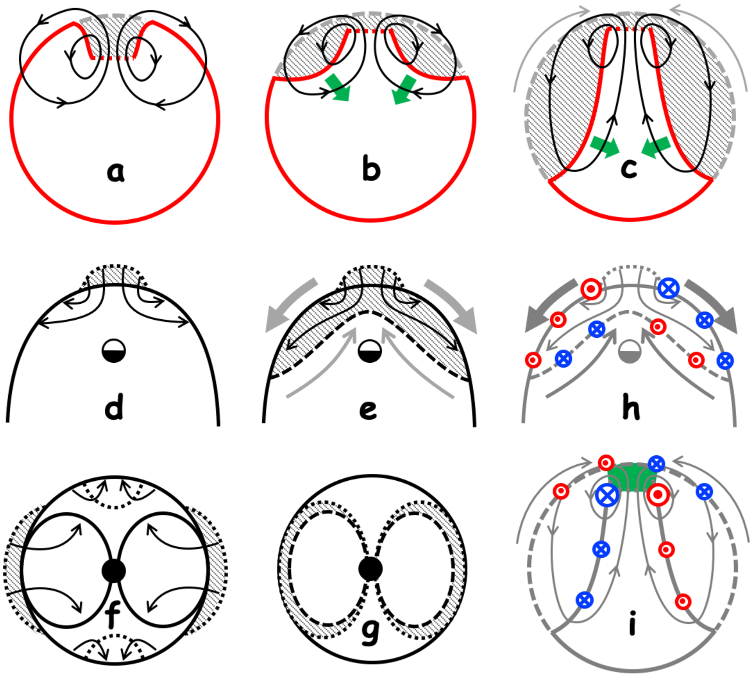

Figure 3. (a) to (c) Our proposed model for the formation of horse-collar auroras by dual-lobe reconnection, in a similar format to Fig. 2d-f. The shaded region indicates newly-closed flux produced by DLR, which is redistributed to dawn and dusk. As time progresses, the OCB moves polewards at dawn and dusk to assume a teardrop shape. The main auroral oval remains relatively unchanged, located equatorward of the circular outline. Flows associated with a viscous solar wind interaction, if it occurs, are indicated by grey arrows. (d) The equatorial plane ($Z = 0$) of the magnetosphere. A region of newly-closed flux is appended to the nose of the magnetosphere by DLR; flows are excited within the magnetosphere (arrows) to return the magnetopause to stress balance with the flow of the solar wind (black arrows). (e) As more closed flux is appended, magnetic flux laden with captured solar wind plasma moves to dawn and dusk. Flows associated with a viscous solar wind interaction are shown in grey. (f) The cross-section of the magnetosphere ($X = 0$). The dipolar lines show the separatrix between closed and open flux regions, with open lobe flux at the top and bottom. DLR removes open flux from the north and south (dotted regions) and appends newly-closed flux at the dawn and dusk flanks. Flows are excited to return the magnetosphere to a circular cross-section. (g) The location of the newly-closed, solar wind plasma laden field lines once equilibrium is re-attained. This flux maps to the dawn and dusk horse-collar auroras in the ionosphere. (h) and (i) Expected field-aligned current (FAC) regions associated with the magnetospheric dynamics driven by dual-lobe reconnection in the equatorial plane of the magnetosphere and the ionosphere. These include the NBZ FACs in the dawn and dusk portions of the dayside polar cap. The expected location of cusp spot auroras produced by magnetosheath precipitation downstream of the ionospheric projection of the reconnection site is indicated in green.

2 Observations

We show three intervals of data. In the first, we employ observations of the auroras and ionospheric flows from the Defense Meteorological Satellite Program (DMSP) F16 and F18 satellites. The DMSP satellites are in sun-synchronous orbits roughly aligned with the dawn-dusk meridian near an altitude of 850 km. The Ion Driftmeter (IDM) component of the Special Sensors–Ions, Electrons, and Scintillation thermal plasma analysis package or SSIES (Rich & Hairston, 1994) on F16 and F18 measured the cross-track horizontal ionospheric convection flow at 1 s cadence (approx. 7 km spatial resolution) along the orbit. The Special Sensor Ultraviolet Spectrographic Imager or SSUSI experiment (Paxton et al., 1992), recorded a swath of auroral luminosity, extending sunwards and antisunwards from the orbit, in five wavelength bands. We use observations at 130.4 nm, which measures emissions associated with electron precipitation-induced O I auroral transitions, and the Lyman-Birge-Hopfield short (LBHs) band, 140 to 152 nm, sensitive to emissions produced by soft electron precipitation. Each pass of the polar regions by a DMSP spacecraft takes 15 to 20 mins. We combine these with measurements of the magnetosphere-ionosphere coupling field-aligned currents (FACs) from the Active Magnetosphere and Planetary Electrodynamics Response Experiment (AMPERE), derived from magnetometer measurements onboard the satellites of the Iridium telecommunications constellation (Anderson et al., 2000; Waters et al., 2001; Coxon et al., 2018). FACs are derived on a grid of 24 magnetic local time (MLT) sectors divided into fifty 1°-bins of geomagnetic latitude, at a cadence of 2 mins. We average the FACs over the duration of each DMSP pass.

The lower panel of Figure 4 shows the IMF conditions for the interval, accessed from the National Aeronautics and Space Administration OMNIWeb portal (King & Papitashvili, 2005). The upper panels present a series of passes of the DMSP satellites over the northern and southern hemispheres (NH and SH) on 15 December 2015. The two left-hand columns show the FACs measured by AMPERE in the two hemispheres. The IMF $B_Y - B_Z$ component vector is shown between these panels. Depending on whether the spacecraft pass is over the NH or SH, the orbital track is indicated in one or other of these panels, with the IDM cross-track plasma flow measurements superimposed. To the right are the corresponding auroral observations in the two wavelength bands.

During the interval of interest, 14:43 to 20:40 UT, the magnitude of the IMF varied in the range 7 to 10 nT, and its orientation rotated from southward but B_Y-dominated, to almost purely northward, and back to B_Y-dominated. At the start of the interval, 14:43 UT, the IMF had components $B_Y \approx -5$ and $B_Z \approx -2$ nT. The FAC patterns were dominated by the expected Region 1 and 2 (R1 and R2) current systems (Iijima & Potemra, 1976) and the ionospheric flows were consistent with twin-cell convection with an east-west asymmetry consistent with $B_Y < 0$. The corresponding auroral configuration showed a main auroral oval that was located equatorward of 70° latitude, with an expanded polar cap. The polar cap continued to expand after this time, until a substorm onset occurred around 15:30 UT (not shown). By 16:25 UT, the IMF had components $B_Y \approx -4$ and $B_Z \approx +3$ nT, the polar cap was somewhat contracted from previously (due to the substorm) and the FACs and ionospheric flows were consistent with lobe-stirring (we note that the R1/R2 FACs are strongest at dusk and dawn in the NH and SH, respectively, where the flow shear between open and closed field lines is strongest), which we expect to be driven by single-lobe reconnection.

At 17:29 and 18:20 UT, the IMF rotated to being northward, $B_Y \approx -1$ and $B_Z \approx +7$ nT, before beginning to become B_Y-dominated again, $B_Y \approx -5$ and $B_Z \approx +2$ nT, at 19:11 UT. Especially at 18:20 and 19:20 UT, the FACs had the characteristic NBZ pattern associated with symmetrical lobe reverse cells, though stronger in the SH than the NH due to solar-illumination in the summer hemisphere and enhanced conductance. The ionospheric flows showed sunwards motions in the central polar cap and antisunwards motions in the dawn and dusk sectors, again consistent with lobe reverse cells. (We

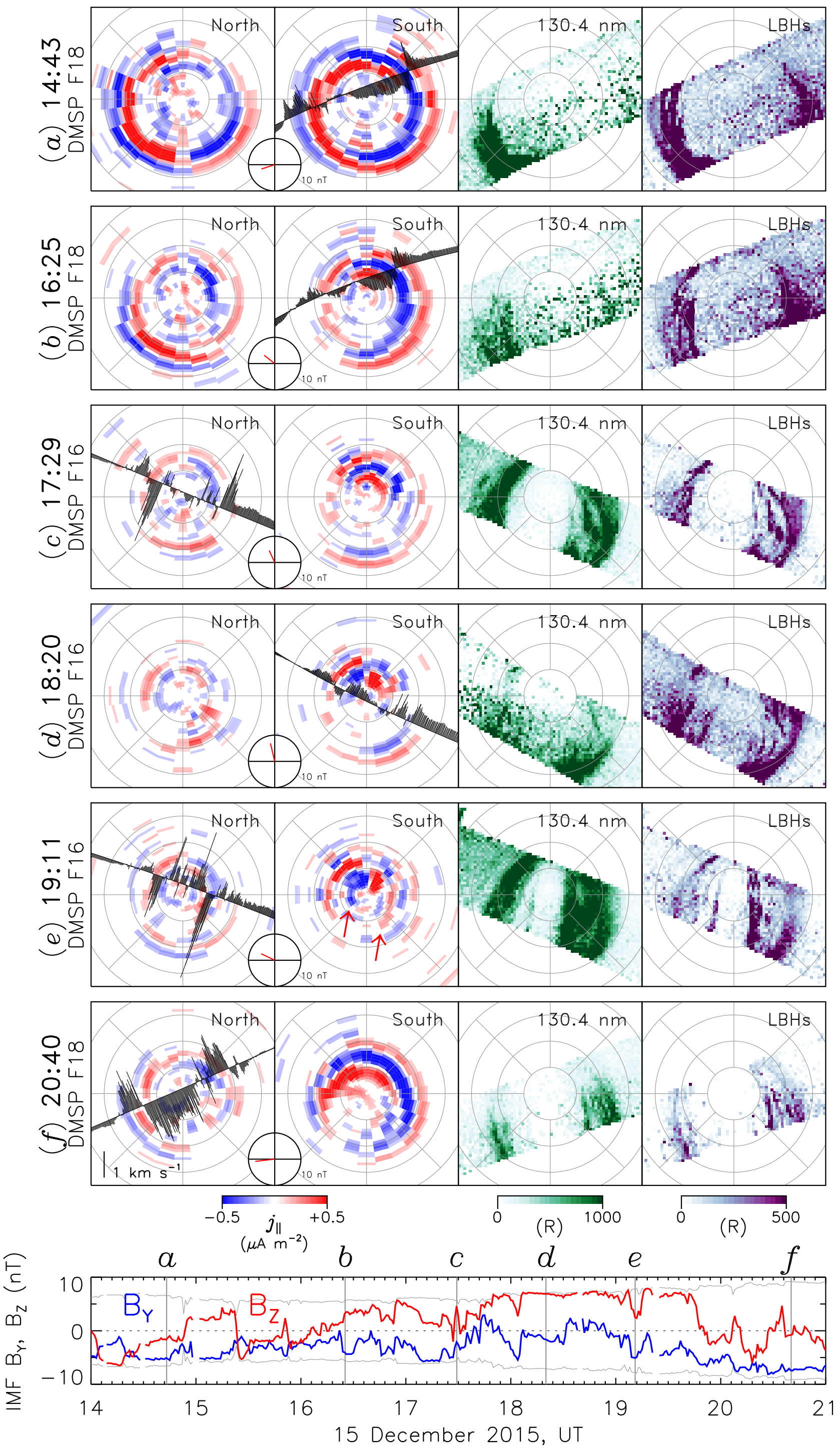

Figure 4. Observations from AMPERE and DMSP F16 and F18 during 15 December 2015, an interval when horse-collar auroras developed, associated with a northward turning of the IMF. Six rows show different passes of the two DMSP spacecraft. On the left is presented the field-aligned currents observed by AMPERE in the northern and southern hemispheres (we suppress $|j_{||}| < 0.1\ \mu\mathrm{A\ m}^{-2}$ to remove noise). Concurrent IMF B_Y and B_Z components are shown in the inset panel, in which the radius of the circle represents 10 nT. The satellite track and cross-track ionospheric flow measured by DMSP/SSIES is displayed over the hemisphere in which the pass occurred. On the right, the corresponding auroras observed by DMSP/SSUSI are displayed. Observations are shown in a geomagnetic latitude and magnetic local time format, with noon to the top and dawn and dusk to the left and right; colatitudes in steps of 10° are represented by circles. The lower panel shows the IMF B_Y (blue) and B_Z (red) components for the interval, together with the total field strength $\pm B_T$ (grey).

note that Reidy et al. (2020) have presented Super Dual Auroral Radar Network (SuperDARN) convection measurements (Chisham et al., 2007) from this interval, see their Figure 10, which corroborate this flow pattern.) Over this period, sun-aligned auroral features appeared poleward of the dawn and dusk sector main oval: the horse-collar auroral configuration that is the subject of this paper. The polar cap became teardrop-shaped and progressively smaller with time as the auroras moved to higher latitudes. At 19:11 UT there was a prominent sun-aligned arc at the poleward edge of the dawn HCA, colocated along much of its length with an upward FAC (indicated by an arrow); a similar downward FAC (second arrow) was colocated with the poleward edge of the dusk HCA and a fainter sun-aligned arc. A key observation is that the sunwards ionospheric flows were located within the dark polar cap, whereas the antisunwards flows were within the dawn and dusk regions of the developing HCA (cf. Fig. 3c). We will argue below that dual-lobe reconnection was occurring during this period, and the HCA are the result of open magnetic flux being closed and redistributed to the dawn and dusk sectors.

By 20:40 UT, the IMF was B_Y-dominated again, asymmetrical twin-cell convection was ongoing, and the opening of magnetic flux by low latitude reconnection had caused the polar cap to re-expand once again.

Next, we present the interval 15 to 21 UT on 1 March 2010. The bottom panel shows the IMF B_Y and B_Z components for the interval. Top panels show passes of the northern and southern hemispheres by DMSP F16, F17, and F18. Emissions in the LBHs band detected by SSUSI are presented (note that the colour scale has been adjusted in individual panels to emphasise weak auroral features), with IDM cross-track drift vectors superimposed when measurements are reliable. At the start of the interval (panel a), $B_Z \approx +5$, $B_Y \approx -5$ nT, the polar cap was empty, and the ionospheric flows were consistent with SLR (see Fig. 2e). Over panels b and c the IMF turned northwards, $B_Z \approx +10$ nT, clock angle $|\theta| < 10°$, and the flows evolved to be sunwards in the central polar cap and antisunwards at dawn and dusk. Horse-collar auroras developed, seen most clearly in panel d, and moved progressively polewards, as seen in panel e. Over the next hour both B_Y and B_Z components changed rapidly, and the flows in the ionosphere became more complicated (panel f); indeed, it is likely that the flow pattern was changing as the spacecraft traversed the polar regions. The IMF clock angle became close to 0° again during panels g and h, and the HCS were still discernible, but they were now displaced, towards dawn in the SH and dusk in the NH. Subsequently the IMF turned to be B_Y-dominated, with $B_Y < 0$, the flow patterns became consistent with lobe-stirring, anticlockwise in the NH (panel l) and clockwise in the SH (panel m) and the arcs moved towards dawn and dusk, respectively. It is possible that the arcs are displaced dawn-dusk to different degrees in the two hemispheres.

We inspected AMPERE and DMSP data for the period 2010 to 2016 (the period that AMPERE data are currently available) for other instances of the formation of horse-collar auroras. Similar sequences of events, purely northward IMF, symmetric NBZ FACs, the development of HCA with sunwards flow in the polar cap and antisunwards flow within the HCA are a common and reproducible feature of the data (indeed, similar observations have been widely reported in the literature, see e.g. Figure 8 of Cumnock and Blomberg (2004), as well as Fig. 10 of Reidy et al. (2020)). We will present a statistical survey of the events in a subsequent paper.

Now, we discuss an interval observed from the Imager for Magnetopause-to-Aurora Global Explorer (IMAGE) spacecraft with the FUV instrument (Mende et al., 2000a, 2000b, 2000c), comprising the Wide-band Imaging Camera (WIC), which mainly measured LBH auroral emissions produced by precipitating electrons, and the Spectrographic Imager (SI12), which observed proton auroras. Horse-collar auroras have not been widely reported in IMAGE observations, and we suspect that the cameras are relatively insensitive to these weak auroral features. The interval of interest is 24 November 2001 during which IMAGE was observing the northern hemisphere, as presented in Figure 6. This

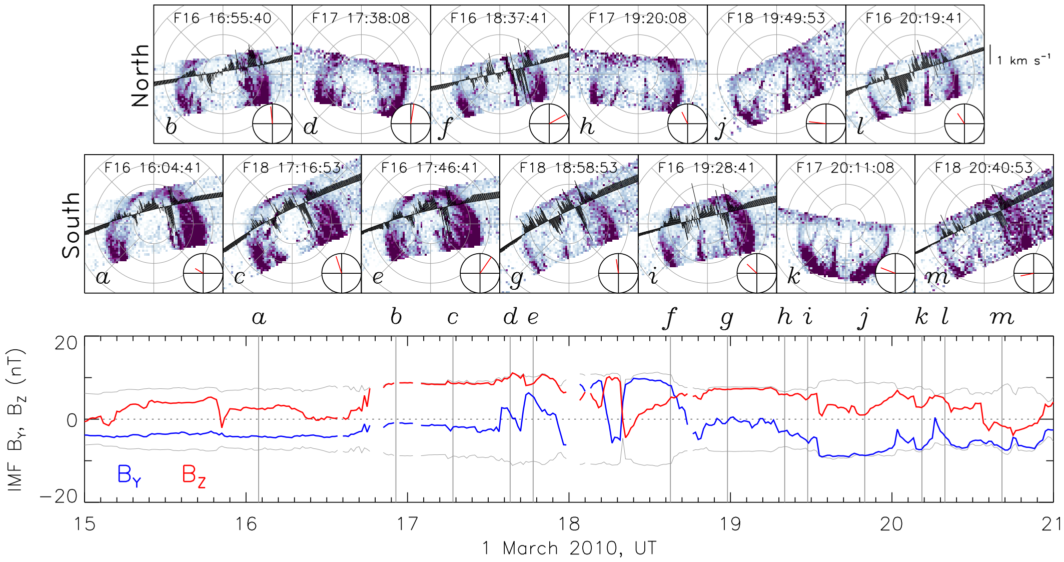

Figure 5. (a) to (m) DMSP/SSIES and DMSP/SSUSI (LBHs emissions) observed by DMSP F16, F17, and F18 on 1 March 2010, presented in a similar format to Fig. 4; passes of the northern and southern hemisphere are shown above and below. (Bottom) The IMF B_Y (blue) and B_Z (red) components, together with the total field strength, $\pm B_T$ (grey).

is an extreme interval, during which the solar wind speed approached 1000 km s^{-1}, the density was variable about an average of 25 cm^{-3}, and the IMF magnitude was near 70 nT. We think that under these conditions DLR created horse-collar auroras that were at the limit of detection by IMAGE.

Panels a and b show the WIC and SI12 observations averaged between 10:20 and 10:30 UT. A prominent cusp spot was observed at this time, a period of strongly northward IMF ($B_Y \approx +14$, $B_Z \approx +51$ nT). DMSP F13 passed across this cusp feature, recording sunwards flows of 2 km s^{-1} colocated with the spot (corresponding to a voltage of approximately 80 kV) and antisunwards flows of 1 km s^{-1} either side (IDM on DMSP F13 had a temporal cadence of 4 s corresponding to a measurement every 28 km). Although we might expect horse-collar auroras to be forming or have formed at this time (as per the previous examples), there is little evidence for them. However, a weak (in comparison to the brighter main oval) auroral arc was associated with the dawn-side edge of the cusp spot in the WIC image (indicated by an arrow), and there was weak auroral emission in the high latitude dawn sectors was observed by both cameras. An hour later (panels c and d), the IMF had rotated to be southwards but B_Y-dominated ($B_Y \approx -40$, $B_Z \approx -23$ nT). DMSP F13 crossed the SH and observed flows consistent with a standard twin-cell convection pattern with the expected dawn-dusk asymmetry (we have mirrored the DMSP track across the noon-midnight meridian to represent the flows as we expect they would appear in the NH). There was no longer a cusp spot, the main auroral oval had moved to low latitudes, and the polar cap had expanded, an indication that low latitude magnetopause reconnection had created new open magnetic flux. As this auroral configuration developed, the dawn and dusk sector weak auroras we expected to see in panels a and b brightened and became more evident (indicated by arrows). These became deformed by the redistribution of magnetic flux in the polar regions represented by the ionospheric flow pattern, being transported antisunwards and dawnwards, with new open flux occupying the dayside polar cap.

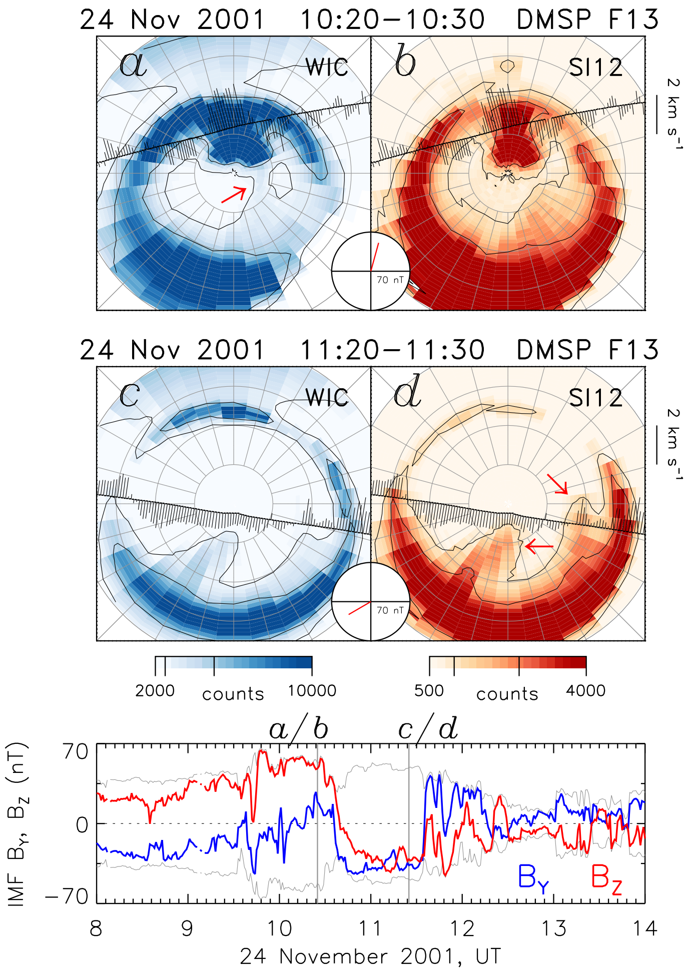

Figure 6. Images of the northern hemisphere auroras observed by WIC and SI12 onboard IMAGE during two periods, 10:20 to 10:30 and 11:20 to 11:30, on 24 November 2001. Two contours are added on the emissions to guide the eye. The inset panel shows the B_Y and B_Z components of the IMF, in which the radius of the circle represents 70 nT. Superimposed is the satellite track and cross-track ionospheric flow measured by DMSP/SSIES onboard DMSP F13. In the top panels, F13 overpasses the northern hemisphere; in the bottom panels the pass is in the southern hemisphere, and the track and flow measurements have been mirrored about the noon-midnight meridian, to reflect the sense of the convection expected in the northern hemisphere. The lower panel shows the IMF B_Y (blue) and B_Z (red) components for the interval; the total magnetic field strength, B_T, is shown in grey.

3 Discussion

During southward IMF ($B_Z < 0$), dayside reconnection creates open magnetic flux which forms the magnetotail lobes; subsequently, nightside reconnection closes flux which returns to the dayside, leading to the Dungey cycle of convection (Dungey, 1961). As described by the expanding/contracting polar cap model of magnetospheric and ionospheric convection (Cowley & Lockwood, 1992; Milan, 2015), the amount of open magnetic flux in the magnetosphere, which dictates the size of the polar cap, is a competition between the rates of dayside and nightside reconnection (Milan et al., 2007); at all times the polar cap remains approximately circular due to the pressure of the solar wind on the magnetopause, the main motivating force for the redistribution of magnetic flux within the magnetosphere. Figure 2d shows the expected ionospheric flow pattern and expansion of the polar cap for dayside but no nightside reconnection.

When $B_Z > 0$ and $B_Y \neq 0$, single-lobe reconnection (SLR) merges the IMF with open magnetic flux of the lobes to create a new open lobe field lines, the open flux content remains unchanged, and the flux within the polar cap is stirred, as shown in Fig. 3e, forming a major "reverse convection cell" with possibly a second, minor cell. The polar cap tends to remain circular, but processes can give rise to auroral features poleward of the main oval, sometimes associated with open field lines, and sometimes closed (see discussion in the Introduction).

In this paper, we specifically discuss the behaviour when $B_Z > 0$ and $B_Y \approx 0$, clock angles $\theta \approx 0°$, when dual-lobe reconnection (DLR) is expected to occur. Now open field lines of the lobes are closed and result in new closed flux draped over the dayside magnetopause. Chisham et al. (2004) and Imber et al. (2006) reasoned that this should result in convection flows sunwards across the dayside open/closed field line boundary or OCB (synonymous with the polar cap boundary) and a general contraction of the polar cap to higher latitudes; the scenario they suggested is shown in Fig. 2f, essentially the reverse of the situation suggested by Cowley and Lockwood (1992) for southward IMF (Fig. 2d). Imber et al. (2006, 2007) and Marcucci et al. (2008) did indeed find instances of the expected flows, but significant contraction of the polar cap was not evident. In this study, we argue that the true signature of polar cap contraction was missed by previous workers because the OCB does not move polewards equally at all local times, but does so predominantly at dawn and dusk to create the teardrop shape associated with horse-collar auroras. We suggest that this occurs progressively, as indicated in Fig. 3, panels a to c.

Fig. 3a shows that a region of dayside open flux has been closed by DLR, exciting sunward convection flows across the reconnecting portion of the OCR (dotted), which turn dawnwards and duskwards due to the magnetic tension force and the flow of the magnetosheath. The ionospheric convection pattern requires interchange flows to close the streamlines, leading to polar cap motions excited by stresses imposed on the magnetopause by the pressure of the solar wind (see below). Where the streamlines cross "adiaroic" portions of the OCB (away from the reconnecting portion of the boundary (Siscoe & Huang, 1985)) the flows and boundary move together, carrying the OCB polewards (Fig. 3b, green arrows), beginning to form a teardrop-shaped polar cap. As open flux continues to be closed the the poleward motion of the OCB progresses around the flanks of the polar cap (Fig. 3c). The newly-closed magnetic flux now occupies the high latitude dawn and dusk sectors, and particle precipitation on these field lines creates the horse-collar auroral configuration. As DLR continues, the polar cap will continue to shrink, with the HCAs expanding to ever-higher latitudes. Non-zero B_Y could lead to differences in the convection in the dawn and dusk reverse cells and hence asymmetries in the size of the dawn and dusk HCA regions, subject to the constraint that the amount of newly-closed flux at dawn is equal in both northern and southern hemispheres, with the same applying to dusk.

The associated flows in the equatorial plane of the magnetosphere ($Z = 0$) are illustrated in Fig. 3d and e, whereas panels f and g show the $X = 0$ plane. Fig. 3d corresponds to the situation in Fig. 3a: a pulse of DLR has created a region of closed magnetic flux draped across the dayside magnetosphere (dotted outline and shaded region). The magnetopause is no longer in magnetohydrodynamic stress balance with the flow of the solar wind, and motions are excited within the magnetosphere to return it to a stream-lined bullet shape. As DLR continues, Fig. 3e, the dayside region of the magnetosphere becomes increasingly occupied by newly-closed flux (demarcation between old and new closed flux indicated by dashed line), and this will begin to be pushed antisunwards around the flanks. This antisunwards progression may be aided by viscous processes associated with the flow of the solar wind (thick grey arrows); in this case, return flows will be required in the inner magnetosphere (thin grey arrows). Fig. 3f shows the magnetospheric configuration before DLR, with a circular cross-section and an approximately dipolar field-shaped boundary separating the open lobes and closed field line regions. After DLR, the lobes are eroded at the top and the bottom, and new regions of closed field lines are appended at the dawn and dusk flanks (dotted lines). Flows are excited to return the magnetopause to an approximately circular cross-section, these flows mapping to the ionosphere to produce the patterns indicated in Fig. 3a to c. Fig. 3g shows the resulting cross-section, in which the lobes have shrunk, the dotted line indicating the new separatrix between open and closed field lines, and the dashed line indicating the demarcation between old and new closed flux. The newly-closed flux between the dotted and dashed lines maps to the location of the horse-collar auroras.

Field-aligned currents (FACs) are required to couple the magnetospheric and ionospheric phenomena described above, illustrated in the equatorial plane of the magnetosphere (Fig. 3h) and in the ionosphere (Fig. 3i). Blue and red circles indicate FACs into and out of the page, respectively. The vorticity of the reverse lobe convection cells requires a pair of upward and downward FACs, the familiar NBZ current system; this current system will be extended along the convection reversal boundary along the edges of the horse-collar auroral regions. All these FACs map to the magnetopause and can close across the nose of the magnetosphere through a dawn-to-dusk current, in a similar manner to the usual Chapman-Ferraro current. FACs will also be generated due to pressure gradients in the inner magnetosphere near the boundary between new and old closed flux (in a similar manner to usual Region 2 FACs) and will close through a dayside partial ring current. These FACs will map equatorward of the NBZ currents in the ionosphere, corresponding to the convection shear at the equatorward edge of the lobe cells (and any viscous flows, should they be present). Auroras might be expected to be produced in the ionosphere at the foot of upward FACs, produced by precipitating electrons. Auroras are known to be colocated with the upward NBZ FAC, known as high-latitude detached auroras or HiLDAs (Frey, 2007; Carter et al., 2018). Fig. 3i also shows where auroras can form (green) due to direct precipitation of magnetosheath plasma downstream (sunward) of the footprint of the lobe reconnection site, to form an auroral cusp spot (Milan et al., 2000; Frey et al., 2002; Carter et al., 2020), which would be accompanied by a reverse ion dispersion signature (Woch & Lundin, 1992). The FAC pattern also indicates that auroras might be expected along the poleward edge of the dawn horse-collar region.

Now we compare the model predictions with the observations. The ionospheric flow pattern presented in Fig. 3c, with sunwards convection in the polar cap and antisunwards convection in the region of weak horse-collar auroras, agrees with the observations in Figs. 4 and 5. Symmetric NBZ FACs seen by AMPERE, and the SuperDARN flows reported by Reidy et al. (2020), corroborate that reverse lobe cells are present at the sunward portion of the HCAs. The model also predicts the progressive evolution of the polar cap from circular to teardrop-shaped, which is a well-known feature of periods of horse-collar auroras. The location of the cusp spot predicted in Fig. 3i agrees with Fig. 6a and b.

Flow shears have long been implicated in the formation of PCAs (e.g., Cumnock & Blomberg, 2004). However, when it was assumed that these flow shears occurred within the open polar cap, it was unclear why the shears should be sharp enough to produce thin auroral arcs, and as long-lived as observations suggested. The model presented here places these flow shears at the boundary between open and closed field lines, hence necessarily producing the required spatial and temporal behaviour. Although we should be careful not to over-interpret the observations, we note elongated, sun-aligned upward and downward FAC regions in Fig. 4e, indicated by arrows, that are close to the flow reversals in the driftmeter data, as predicted in Fig. 3i, and that are colocated with the brightest emissions at the poleward edges of the dawn and dusk HCAs. A similar, albeit faint, dawn arc is also seen in Fig. 6a. Hence, the model also explains why polar cap arcs often form adjacent to regions of particle precipitation characteristic of trapped plasma on closed magnetic field lines, in other words, a thickened plasma sheet at dawn and dusk (e.g., Meng, 1981; Newell et al., 2009; Cumnock et al., 2002).

Dual-lobe reconnection has been postulated to be an efficient mechanism by which the magnetosphere can capture cold dense solar wind plasma (e.g., Sandholt et al., 1999; Imber et al., 2006). The horse-collar region will then be associated with trapped dense plasma, which may give rise to weak or sub-visual auroral emission. This also places a distinct boundary between regions of dissimilar plasmas (hot, tenuous and cold, dense) within the magnetosphere, and could be related to observations of a low-latitude boundary layer adjacent to the flank magnetopause during periods of northwards IMF (Scholer & Treumann, 1997). This internal boundary could be prone to an interchange instability or the Kelvin-Helmholtz instability (KHI), which could corrugate the boundary and give rise to structured auroral emission within the horse-collar region (as shown in Fig. 1). The KHI can also operate on the magnetopause, and it was recently suggested by Q.-H. Zhang et al. (2020) that this can give rise to flow shears that propagate into the magnetosphere and produce multiple polar cap arcs; the present model elucidates why closed magnetic flux is to be found at high latitudes, within which such arcs can form.

It has been further suggested that this captured solar wind plasma can contribute to the formation of a cold, dense plasma sheet or CDPS (Terasawa et al., 1997; Øieroset et al., 2005; Imber et al., 2006; Wing et al., 2006), though tracking the redistribution of this plasma in the magnetosphere was thought difficult (Fuselier et al., 2015). Here we argue that the HCAs represent the regions of trapped solar wind plasma and by charting their development, this redistribution can be tracked. Once the plasma has been transported to the tail, mixing with the pre-existing plasma sheet is thought to occur, though the mechanism by which this is achieved is unclear. Potentially the KHI and interchange processes taking place at the boundary between the new and old closed flux contribute to this mixing, and could be revealed by small-scale auroral or convection features in the ionosphere.

Convection measurements in the nightside polar regions during northward IMF regularly reveal disordered flows with multiple sunwards/antisunwards flows shears; as discussed above, these flow shears could be associated with the formation of sun-aligned arcs in both the open and closed field line regions. These disordered motions could be a signature of the mixing processes described previously, superimposed on the large-scale flows shown in Fig. 3c. These observations also suggest that the excitation of convection associated with DLR, especially on the nightside is a haphazard affair. The main driver of convection is the pressure of the solar wind exerted on the magnetosphere and the redistribution of magnetic flux within to achieve stress balance at the magnetopause (Cowley & Lockwood, 1992). DLR is associated with the removal of flux from the magnetotail lobes (Fig. 3f), and this may manifest itself as sporadic and spatially incoherent polar cap flows.

In Figure 7b and c we illustrate how we expect the auroral morphology to evolve after a southwards turning of the IMF. Panel a shows the pre-existing horse-collar con-

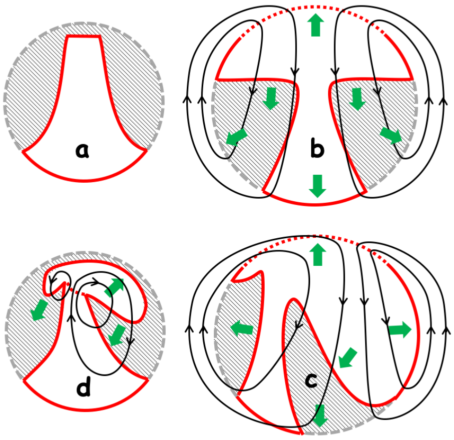

Figure 7. Anticipated response to a change in IMF orientation of (a) the original polar cap and horse-collar configuration. (b) A southward turning leads to the addition of new open flux to the dayside polar cap by low latitude magnetopause reconnection, causing an expansion of the main auroral oval and a general antisunwards motion of the horse-collar regions within the twin-cell convection pattern. (c) A similar situation but with $B_Y > 0$ (shown for NH), leads to the asymmetrical addition of new open flux and a general duskwards motion of the closed flux at high latitudes. (d) Continued northwards IMF but with $B_Y > 0$ drives single-lobe reconnection which siphons open flux from the pre-existing polar cap and expands a new polar cap at dawn (and maybe a smaller one at dusk), causing closed flux to move together and duskwards (in the NH).

figuration. The onset of low latitude magnetopause reconnection will lead to the creation of new open flux which will be appended to the dayside polar cap, abutting the dayside portion of the HCA (Fig. 7b). As this region expands, there will be a general expansion of the main oval to lower latitudes, and a redistribution of open and closed flux at higher latitudes, in the form of a twin-cell convection pattern, that pushes the HCA regions towards the nightside (cf. Fig. 8c of Milan et al. (2005)). If the convection pattern has a dawn-dusk asymmetry associated with a non-zero IMF B_Y (Fig. 7c), then the regions will be deformed as seen in Fig. 6c and d (cf. Newell & Meng, 1995; Goudarzi et al., 2008). Fig. 7d sketches the evolution expected if the IMF remains northwards but develops a non-zero B_Y (specifically shown in the NH for $B_Y > 0$): now the open flux content of the magnetosphere remains unchanged, but single-lobe reconnection siphons open flux from the pre-existing polar cap and produces a new region of open flux at dawn (Milan et al., 2005); it is also possible that if a second, smaller reverse cell is present (Fig. 2e) then a smaller open region at dusk could also form. SLR can occur at different rates in the two hemispheres, so arc motions in the NH and SH driven by this process can be independent of each other (see Fig. 5). Considerations such as these can be used to explain many of the auroral configurations and evolutions reported in the literature, for instance in the examples reported in Cumnock and Blomberg (2004).

As we have shown, the horse-collar auroras are likely associated with a sun-aligned arc at the poleward boundary of the dawn sector closed flux. The regions of HCAs tend also to be filled with multiple sun-aligned arcs (see Fig. 1). Mechanisms have been proposed that lead to (sometimes multiple) small-scale flow shears in both open and closed field line regions, which could drive FACs and hence produce auroras (e.g., Q.-H. Zhang et al., 2020). It is anticipated that the response of the polar regions to changes in the IMF, sketched in Fig. 7, can explain the motions of such arcs. The mechanism proposed by Milan et al. (2005) to produce TPAs via nightside reconnection can also operate, though this will be confined to the open polar cap region. This mechanism would likely form TPAs adjacent to the horse-collar auroras if they have developed previously, and this could influence the range of local times at which TPAs are initially seen. The subsequent motion of a TPA is associated with changes in polarity of the B_Y component of the IMF (Valladares et al., 1994; Milan et al., 2005), suggesting conditions that are not favourable for DLR and the formation of horse-collar auroras, so again Fig. 7 encompasses many of possible configurations that can arise. As the IMF tends to undergo changes in orientation on timescales of minutes and hours and the lobe reconnection sites will move around, at some times undergoing DLR and at others SLR, we can expect a very complicated distribution of open and closed magnetic flux to develop in the polar regions. This could take the form of a complex interleaving of regions of open and closed magnetic flux in the dawn and dusk regions, perhaps resembling the spatial distribution of multiple sun-aligned arcs. (This could also explain the mixture of open and closed particle populations in the NBZ low-latitude boundary layer.) As asserted by Fear et al. (2015), an understanding of how lobe reconnection interacts with both open and closed flux on the magnetopause is important for understanding all the magnetic geometries and structures that can arise.

We finally note that a key prediction of the model proposed, for the formation of the HCS by DLR and the subsequent motions of features by SLR or low latitude reconnection, is that the timescales involved are dependent on the reconnection rates. If an arc system is created solely by a convection reversal boundary, then in principle, in response to a change in the B_Y component of the IMF, that convection reversal can fade away and a new shear flow can form somewhere else in the polar cap almost instantaneously, in which case arcs could jump from one location to another. Observationally, PCA systems tend to move as a coherent feature, suggesting that they are associated with a long-lived magnetic structure (such as a region of closed flux). A quiet-time polar cap tends to contain less than 0.5 GWb of open flux (e.g., Milan et al., 2005, 2007). To close half of that, say 0.2 GWb, by DLR to form HCAs at a reconnection rate of 80 kV (Fig. 6), would take 40 mins. A lobe reconnection rate of 80 kV seems atypically high (and does occur during an interval of $B_Z \approx +50$ nT!), but it is not unprecedented (Clauer et al., 2016). However, timescales of 1 to 2 hours might be more usual. Equally, the timescale for a TPA to move from one side of the polar cap to the other through lobe-stirring associated with SLR, should be of the order of an hour or more, consistent with observations (e.g., Milan et al., 2005).

4 Conclusions

We have described how dual-lobe reconnection occurring during periods of strongly northward IMF ($B_Z > 0$, $B_Y \approx 0$) can give rise to the formation of the common horse-collar auroral configuration, in which the polar cap becomes teardrop-shaped and weak auroras move to high latitudes in the dawn and dusk sectors. This naturally explains many of the features of the northwards-IMF magnetosphere, including the capture of solar wind plasma by the magnetosphere and the formation of a low-latitude boundary layer and a cold, dense plasma sheet. This model provides a new understanding of the structure and dynamics of the magnetosphere, resolving many long-standing questions.

Once the HCA has formed, changes in the orientation of the IMF can lead to a number of different evolutions of the system, depending on whether high or low latitude magnetopause reconnection takes place and the B_Y component of the IMF. The creation of new open flux, or the redistribution of existing open flux, can lead to antisunwards and/or east-west motions of auroral features, as open and closed flux regions alike are stirred within the polar regions. With changeable IMF, a complicated magnetic structure can arise.

Our model is an extension of the expanding/contracting polar cap (ECPC) model first proposed in full by Cowley and Lockwood (1992), originally developed to explain the dynamics of the magnetosphere in response to low latitude magnetopause reconnection (occurring for $B_Z < 0$) and substorm-related tail reconnection. This model was augmented by Milan et al. (2005) to show how magnetotail reconnection within a twisted tail ($B_Z > 0$, $B_Y \neq 0$) could give rise to tongues of closed magnetic flux intruding into the polar cap from the nightside to form transpolar arcs. Carter et al. (2015) explained how low latitude magnetopause reconnection occurring for B_Y-dominated IMF ($B_Z \approx 0$, $B_Y \neq 0$) gives rise to a class of polar cap auroras known as bending arcs. We have now elucidated the dynamics during purely-northwards IMF, completing our understanding of the ECPC response of the magnetosphere to solar wind coupling under all IMF clock angle regimes.

There still remains much to understand. Several future studies are anticipated. We will investigate the clock angle range over which horse-collar auroras develop, to better understand the DLR process. We will study the temporal development of the HCA from the initial northward-turning of the IMF to quantify the rate at which magnetic flux is closed by DLR. We will also use the evolution of the HCA to track the capture of solar wind plasma by the magnetosphere, its transport within the magnetosphere, and its link to the formation of the cold, dense plasma sheet.

Acknowledgments

SEM, JAC, and SMI are supported by the Science and Technology Facilities Council (STFC), UK, grant no. ST/S000429/1. GEB is supported by an STFC studentship. MRH was supported by the National Science Foundation under grant AGS-1929866 and by NASA under grant 80NSSC20K1071. The work at the Birkeland Centre for Space Science is supported by the Research Council of Norway under contract 223252/F50. BH is supported by the Belgian National Fund for Scientific Research (FNRS). We acknowledge use of NASA/GSFC's Space Physics Data Facility's CDAWeb service (at `http://cdaweb.gsfc.nasa.gov`), and OMNI data. The OMNI data and the IMAGE WIC and SI12 data were obtained from CDAWeb (`https://cdaweb.gsfc.nasa.gov`). The DMSP/SSUSI file type EDR-AUR data were obtained from `http://ssusi.jhuapl.edu` (data version 0106, software version 7.0.0, calibration period version E0018). The DMSP/SSIES data were downloaded from the Madrigal Database at Millstone Hill (`http://millstonehill.haystack.mit.edu`). AMPERE data were obtained from `http://ampere.jhuapl.edu`.

References

Anderson, B., Takahashi, K., & Toth, B. (2000). Sensing global Birkeland currents with Iridium® engineering magnetometer data. *Geophysical Research Letters*, *27*(24), 4045–4048.

Axford, W., & Hines, C. (1961). A unifying theory of high-latitude geophysical phenomena and geomagnetic storms. *Canadian Journal of Physics*, *39*(10), 1433–1464.

Burke, W., Gussenhoven, M. S., Kelley, M., Hardy, D., & Rich, F. (1982). Electric and magnetic field characteristics of discrete arcs in the polar cap. *Journal of Geophysical Research: Space Physics*, *87*(A4), 2431–2443.

Carlson, H., & Cowley, S. (2005). Accelerated polar rain electrons as the source of sun-aligned arcs in the polar cap during northward interplanetary magnetic field conditions. *Journal of Geophysical Research: Space Physics*, *110*(A5).

Carter, J., Milan, S., Fear, R., Kullen, A., & Hairston, M. (2015). Dayside reconnection under interplanetary magnetic field By-dominated conditions: The formation and movement of bending arcs. *Journal of Geophysical Research: Space Physics*, *120*(4), 2967–2978.

Carter, J., Milan, S., Fear, R., Walach, M.-T., Harrison, Z., Paxton, L., & Hubert,

B. (2017). Transpolar arcs observed simultaneously in both hemispheres. *Journal of Geophysical Research: Space Physics*, *122*(6), 6107–6120.

Carter, J., Milan, S., Fogg, A., Paxton, L., & Anderson, B. (2018). The association of high-latitude dayside aurora with NBZ field-aligned currents. *Journal of Geophysical Research: Space Physics*, *123*(5), 3637–3645.

Carter, J., Milan, S., Fogg, A., Sangha, H., Lester, M., Paxton, L., & Anderson, B. (2020). The evolution of long-duration cusp spot emission during lobe reconnection with respect to field-aligned currents. *Journal of Geophysical Research: Space Physics*, *125*, e2020JA027922.

Chisham, G., Freeman, M., Coleman, I., Pinnock, M., Hairston, M., Lester, M., & Sofko, G. (2004). Measuring the dayside reconnection rate during an interval of due northward interplanetary magnetic field. *Annales Geophysicae*, *22*(12), 4243–4258.

Chisham, G., Lester, M., Milan, S. E., Freeman, M., Bristow, W., Grocott, A., ... others (2007). A decade of the Super Dual Auroral Radar Network (SuperDARN): Scientific achievements, new techniques and future directions. *Surveys in geophysics*, *28*(1), 33–109.

Clauer, C. R., Xu, Z., Maimaiti, M., Ruohoneimi, J. M., Scales, W., Hartinger, M. D., ... Lopez, R. E. (2016). Investigation of a rare event where the polar ionospheric reverse convection potential does not saturate during a period of extreme northward IMF solar wind driving. *Journal of Geophysical Research: Space Physics*, *121*(6), 5422–5435.

Cowley, S. (1981). Magnetospheric and ionospheric flow and the interplanetary magnetic field. *The Physical Basis of the Ionosphere in the Solar-Terrestrial System, AGARD-CP-295*, (4-1)–(4-14).

Cowley, S., & Lockwood, M. (1992). Excitation and decay of solar wind-driven flows in the magnetosphere-ionosphere system. *Annales Geophysicae*, *10*, 103–115.

Coxon, J., Milan, S., & Anderson, B. (2018). A review of Birkeland current research using AMPERE. *Electric currents in geospace and beyond*, 257–278.

Craven, J., Murphree, J., Frank, L., & Cogger, L. (1991). Simultaneous optical observations of transpolar arcs in the two polar caps. *Geophysical Research Letters*, *18*(12), 2297–2300.

Cumnock, J., & Blomberg, L. (2004). Transpolar arc evolution and associated potential patterns. *Annales Geophysicae*, *22*(4), 1213–1231.

Cumnock, J., Sharber, J., Heelis, R., Blomberg, L. G., Germany, G., Spann, J., & Coley, W. (2002). Interplanetary magnetic field control of theta aurora development. *Journal of Geophysical Research: Space Physics*, *107*(A7), SIA–4.

Dungey, J. (1961). Interplanetary magnetic field and the auroral zones. *Physical Review Letters*, *6*(2), 47.

Dungey, J. (1963). The structure of the exosphere, or adventures in velocity space. *Geophysics, The Earth's Environment*.

Fear, R. (2019). The northward IMF magnetosphere. *AGU Centennial monograph, in press*.

Fear, R., & Milan, S. (2012a). The IMF dependence of the local time of transpolar arcs: Implications for formation mechanism. *Journal of Geophysical Research: Space Physics*, *117*(A3).

Fear, R., & Milan, S. (2012b). Ionospheric flows relating to transpolar arc formation. *Journal of Geophysical Research: Space Physics*, *117*(A9).

Fear, R., Milan, S., Carter, J., & Maggiolo, R. (2015). The interaction between transpolar arcs and cusp spots. *Geophysical Research Letters*, *42*(22), 9685–9693.

Fear, R., Milan, S., Maggiolo, R., Fazakerley, A., Dandouras, I., & Mende, S. (2014). Direct observation of closed magnetic flux trapped in the high-latitude magnetosphere. *Science*, *346*(6216), 1506–1510.

Frank, L., Craven, J., Burch, J., & Winningham, J. (1982). Polar views of the

Earth's aurora with Dynamics Explorer. *Geophysical Research Letters*, *9*(9), 1001–1004.

Frey, H. (2007). Localized aurora beyond the auroral oval. *Reviews of Geophysics*, *45*(1).

Frey, H., Mende, S., Immel, T., Fuselier, S., Claflin, E., Gérard, J.-C., & Hubert, B. (2002). Proton aurora in the cusp. *Journal of Geophysical Research: Space Physics*, *107*(A7), SMP–2.

Fuselier, S., Dayeh, M., Livadiotis, G., McComas, D., Ogasawara, K., Valek, P., … Petrinec, S. (2015). Imaging the development of the cold dense plasma sheet. *Geophysical Research Letters*, *42*(19), 7867–7873.

Fuselier, S., Petrinec, S., Trattner, K., & Lavraud, B. (2014). Magnetic field topology for northward imf reconnection: Ion observations. *Journal of Geophysical Research: Space Physics*, *119*(11), 9051–9071.

Goudarzi, A., Lester, M., Milan, S., & Frey, H. (2008). Multi-instrumentation observations of a transpolar arc in the northern hemisphere. *Annales Geophysicae*, *26*(1), 201–210.

Hardy, D., Burke, W., & Gussenhoven, M. (1982). DMSP optical and electron measurements in the vicinity of polar cap arcs. *Journal of Geophysical Research: Space Physics*, *87*(A4), 2413–2430.

Hones Jr, E., Craven, J., Frank, L., Evans, D., & Newell, P. (1989). The horse-collar aurora: A frequent pattern of the aurora in quiet times. *Geophysical Research Letters*, *16*(1), 37–40.

Hosokawa, K., Kullen, A., Milan, S., Reidy, J., Zou, Y., Frey, H. U., … Fear, R. (2020). Aurora in the polar cap: A review. *Space Science Reviews*, *216*(1), 15.

Iijima, T., & Potemra, T. (1976). The amplitude distribution of field-aligned currents at northern high latitudes observed by Triad. *Journal of Geophysical Research*, *81*(13), 2165–2174.

Imber, S., Milan, S., & Hubert, B. (2006). The auroral and ionospheric flow signatures of dual lobe reconnection. *Annales Geophyiscae*, *24*(11), 3115–3129.

Imber, S., Milan, S., & Hubert, B. (2007). Observations of significant flux closure by dual lobe reconnection. *Annales Geophysicae*, *25*, 1617–1627.

King, J., & Papitashvili, N. (2005). Solar wind spatial scales in and comparisons of hourly Wind and ACE plasma and magnetic field data. *Journal of Geophysical Research: Space Physics*, *110*(A2).

Kullen, A., Brittnacher, M., Cumnock, J., & Blomberg, L. (2002). Solar wind dependence of the occurrence and motion of polar auroral arcs: A statistical study. *Journal of Geophysical Research: Space Physics*, *107*(A11), 13–1.

Kullen, A., Fear, R., Milan, S. E., Carter, J., & Karlsson, T. (2015). The statistical difference between bending arcs and regular polar arcs. *Journal of Geophysical Research: Space Physics*, *120*(12), 10–443.

Marcucci, M., Coco, I., Ambrosino, D., Amata, E., Milan, S., Bavassano Cattaneo, M., & Retinò, A. (2008). Extended SuperDARN and IMAGE observations for northward IMF: Evidence for dual lobe reconnection. *Journal of Geophysical Research: Space Physics*, *113*(A2).

Mende, S., Heetderks, H., Frey, H., Lampton, M., Geller, S., Abiad, R., … others (2000b). Far ultraviolet imaging from the IMAGE spacecraft. 2. Wideband FUV imaging. *Space Science Reviews*, 271–285.

Mende, S., Heetderks, H., Frey, H., Lampton, M., Geller, S., Habraken, S., … others (2000a). Far ultraviolet imaging from the IMAGE spacecraft. 1. System design. *Space Science Reviews*, *91*(1-2), 243–270.

Mende, S., Heetderks, H., Frey, H., Stock, J., Lampton, M., Geller, S., … others (2000c). Far ultraviolet imaging from the image spacecraft. 3. spectral imaging of Lyman-α and OI 135.6 nm. *Space Science Reviews*, 287–318.

Meng, C.-I. (1981). Polar cap arcs and the plasma sheet. *Geophysical Research Letters*, *8*(3), 273–276.

Milan, S. (2015). Sun et lumière: Solar wind-magnetosphere coupling as deduced from ionospheric flows and polar auroras. In *Magnetospheric Plasma Physics: The Impact of Jim Dungey's Research* (pp. 33–64). Springer.

Milan, S., Carter, J., & Hubert, B. (2020). Probing the magnetic structure of a pair of transpolar arcs with a solar wind pressure step. *Journal of Geophysical Research: Space Physics*, *125*(2), e2019JA027196.

Milan, S., Hubert, B., & Grocott, A. (2005). Formation and motion of a transpolar arc in response to dayside and nightside reconnection. *Journal of Geophysical Research: Space Physics*, *110*(A1).

Milan, S., Lester, M., Cowley, S., & Brittnacher, M. (2000). Dayside convection and auroral morphology during an interval of northward interplanetary magnetic field. *Annales Geophysicae*, *18*(4), 436–444.

Milan, S., Provan, G., & Hubert, B. (2007). Magnetic flux transport in the Dungey cycle: A survey of dayside and nightside reconnection rates. *Journal of Geophysical Research: Space Physics*, *112*(A1).

Newell, P. T., Liou, K., & Wilson, G. R. (2009). Polar cap particle precipitation and aurora: Review and commentary. *Journal of Atmospheric and Solar-Terrestrial Physics*, *71*(2), 199–215.

Newell, P. T., & Meng, C.-I. (1995). Creation of theta-auroras: The isolation of plasma sheet fragments in the polar cap. *Science*, *270*(5240), 1338–1341.

Øieroset, M., Raeder, J., Phan, T., Wing, S., McFadden, J., Li, W., ... Balogh, A. (2005). Global cooling and densification of the plasma sheet during an extended period of purely northward IMF on October 22–24, 2003. *Geophysical Research Letters*, *32*(12).

Østgaard, N., Mende, S., Frey, H., Frank, L., & Sigwarth, J. (2003). Observations of non-conjugate theta aurora. *Geophysical Research Letters*, *30*(21).

Paxton, L., Meng, C.-I., Fountain, G., Ogorzalek, B., Darlington, E., Gary, S., ... others (1992). Special sensor ultraviolet spectrographic imager: An instrument description. In *Instrumentation for planetary and terrestrial atmospheric remote sensing* (Vol. 1745, pp. 2–15).

Reidy, J., Fear, R., Whiter, D., Lanchester, B., Kavanagh, A., Milan, S., ... Zhang, Y. (2018). Interhemispheric survey of polar cap aurora. *Journal of Geophysical Research: Space Physics*, *123*(9), 7283–7306.

Reidy, J., Fear, R., Whiter, D., Lanchester, B., Kavanagh, A., Price, D., ... Paxton, L. (2020). Multi-scale observation of two polar cap arcs occurring on different magnetic field topologie. *Journal of Geophysical Research: Space Physics*, *125*, in press.

Reiff, P. (1982). Sunward convection in both polar caps. *Journal of Geophysical Research: Space Physics*, *87*(A8), 5976–5980.

Reiff, P., & Burch, J. (1985). Imf by-dependent plasma flow and birkeland currents in the dayside magnetosphere: 2. a global model for northward and southward imf. *Journal of Geophysical Research: Space Physics*, *90*(A2), 1595–1609.

Rich, F., & Hairston, M. (1994). Large-scale convection patterns observed by DMSP. *Journal of Geophysical Research: Space Physics*, *99*(A3), 3827–3844.

Sandholt, P., Farrugia, C., Cowley, S., Denig, W., Lester, M., Moen, J., & Lybekk, B. (1999). Capture of magnetosheath plasma by the magnetosphere during northward IMF. *Geophysical Research Letters*, *26*(18), 2833–2836.

Scholer, M., & Treumann, R. (1997). The low-latitude boundary layer at the flanks of the magnetopause. *Space Science Reviews*, *80*(1-2), 341–367.

Siscoe, G., & Huang, T. (1985). Polar cap inflation and deflation. *Journal of Geophysical Research: Space Physics*, *90*(A1), 543–547.

Taylor, M., Lavraud, B., Escoubet, C., Milan, S., Nykyri, K., Dunlop, M., ... others (2008). The plasma sheet and boundary layers under northward imf: A multi-point and multi-instrument perspective. *Advances in Space Research*, *41*(10), 1619–1629.

Terasawa, T., Fujimoto, M., Mukai, T., Shinohara, I., Saito, Y., Yamamoto, T., ... others (1997). Solar wind control of density and temperature in the near-earth plasma sheet: Wind/geotail collaboration. *Geophysical research letters*, *24*(8), 935–938.

Valladares, C., Carlson Jr, H., & Fukui, K. (1994). Interplanetary magnetic field dependency of stable sun-aligned polar cap arcs. *Journal of Geophysical Research: Space Physics*, *99*(A4), 6247–6272.

Waters, C., Anderson, B., & Liou, K. (2001). Estimation of global field aligned currents using the Iridium® system magnetometer data. *Geophysical Research Letters*, *28*(11), 2165–2168.

Wing, S., Johnson, J., & Fujimoto, M. (2006). Timescale for the formation of the cold-dense plasma sheet: A case study. *Geophysical Research Letters*, *33*(23).

Woch, J., & Lundin, R. (1992). Magnetosheath plasma precipitation in the polar cusp and its control by the interplanetary magnetic field. *Journal of Geophysical Research: Space Physics*, *97*(A2), 1421–1430.

Zhang, Q.-H., Zhang, Y.-L., Wang, C., Lockwood, M., Yang, H.-G., Tang, B.-B., ... others (2020). Multiple transpolar auroral arcs reveal insight about coupling processes in the Earth's magnetotail. *Proceedings of the National Academy of Sciences*, *117*(28), 16193–16198.

Zhang, Y., Paxton, L., Zhang, Q.-H., & Xing, Z. (2016). Polar cap arcs: Sun-aligned or cusp-aligned? *Journal of Atmospheric and Solar-Terrestrial Physics*, *146*, 123–128.

Zhu, L., Schunk, R., & Sojka, J. (1997). Polar cap arcs: a review. *Journal of Atmospheric and Solar-Terrestrial Physics*, *59*(10), 1087 - 1126. doi: https://doi.org/10.1016/S1364-6826(96)00113-7